

EXCITATION FUNCTION FOR THE PRODUCTION OF ^{96}Nb IN THE $^{\text{nat}}\text{Zr}(p,x)$ REACTION

NGUYEN VAN DO^{a,b,c,†}, NGUYEN THANH LUAN^{c,d}, NGUYEN THI HIEN^d,
GUINYUN KIM^d, KIM TIEN THANH^c, PHAM DUC KHUE^e AND BUI VAN LOAT^f

^a*Institute of Theoretical and Applied Research, Duy Tan University, Hanoi 100000, Vietnam*

^b*Faculty of Natural Sciences, Duy Tan University, Da Nang, 550000, Vietnam*

^c*Institute of Physics, Vietnam Academy of Science and Technology, 10 Dao Tan, Hanoi, Vietnam*

^d*Department of Physics, Kyungpook National University, Daegu 41566, Republic of Korea*

^e*Institute for Nuclear Science and Technology, VINATOM, 179 Hoang Quoc Viet, Hanoi, Vietnam*

^f*Department of Nuclear Physics, Faculty of Physics,
VNU University of Science, 334 Nguyen Trai, Hanoi, Vietnam*

E-mail: [†]ngvando2404@gmail.com

Received 16 October 2020

Accepted for publication 15 December 2020

Published 05 January 2021

Abstract. We have measured the excitation function for the production of ^{96}Nb in proton induced reaction on natural zirconium in the energy range of 10.58 MeV to 43.61 MeV. The measurement was performed using a stacked-foil activation method combined with off-line γ -ray spectrometry. The stack containing Zr samples, Cu monitors, and several energy degraders was irradiated at the MC-50 Cyclotron of the Korea Institute of Radiological and Medical Sciences (KIRAM), Korea. The cross section of the $^{\text{nat}}\text{Zr}(p,x)^{96}\text{Nb}$ reaction was extracted from the measured activity of reaction product using an HPGe γ -ray detector. The energy of the proton beam along the stacked foil was calculated using the SRIM-2013 code. The proton beam flux was determined via the $^{\text{nat}}\text{Cu}(p,x)^{62}\text{Zn}$ and $^{\text{nat}}\text{Cu}(p,x)^{65}\text{Zn}$ monitoring reactions. The measured cross sections of the $^{\text{nat}}\text{Zr}(p,x)^{96}\text{Nb}$ reaction as a function of the proton energy are compared with the literature data as well as with the theoretical predictions using the TALYS-1.95 nuclear model code and the TENDL-2019 nuclear data library.

Keywords: $^{\text{nat}}\text{Zr}(p,x)^{96}\text{Nb}$ reaction; Excitation function; Stacked-foil activation method; γ -ray spectroscopy; TALYS-1.95; TENDL-2019 data library.

Classification numbers: 25.40.Kv; 25.40.-h.

I. INTRODUCTION

Cross sections of nuclear reactions caused by charged particles play a very important role in both basic research and applications, in particular for the production of medical isotopes and for testing the validity of theoretical nuclear models. In recent decades, studies of nuclear reactions induced by charged particles, especially protons, have been carried out intensively by both experimental measurements and theoretical calculations [1–5]. The cross-section of the nuclear reactions depends on the energy of the incident projectiles. Therefore, the excitation function of reactions is often measured. The cross section measurements were usually performed using a stacked foil activation technique combined with an off-line γ -ray spectroscopy. The main advantage of this method is that it allows a series of sample and monitor foils to be irradiated simultaneously. The proton energy effective at each foil can be obtained by calculation.

In this work, we report the excitation function for the production of ^{96}Nb on natural zirconium targets bombarded by a proton beam with energies in the range from 10.58 to 43.61 MeV. In the literature, we have found some publications on the excitation function of the $^{\text{nat}}\text{Zr}(p,x)^{96}\text{Nb}$ reaction [6–11]. It has been shown that the consistency between the reported data is good at proton energies below about 10 MeV, but poor at higher energies. In addition, significant difference between the experimental data and theoretical predictions are still observed. Consequently, further measurements of the $^{\text{nat}}\text{Zr}(p,x)^{96}\text{Nb}$ reaction cross sections at energies above 10 MeV are needed to provide additional data for better evaluation and verification of the nuclear model calculations.

As usual, we first measure the excitation function of the $^{\text{nat}}\text{Zr}(p,x)^{96}\text{Nb}$ reaction and then perform theoretical calculations. Since the cross section is derived from the measured activity of the reaction product, activity measurement becomes one of the most important tasks of the activation experiment. For γ -ray activity measurements and data processing, corrections for interference and count loss were made. The obtained cross sections are compared with previous measured data. In addition, calculations were performed using the TALYS-1.95 code and tested with different level density models. Finally, the consistency between theoretical and experimental results is also discussed.

II. EXPERIMENT

The excitation function for the proton induced reaction $^{\text{nat}}\text{Zr}(p,x)^{96}\text{Nb}$ has been measured by using the well-known stacked-foil activation method combined with off-line γ -ray spectrometry. Details of this experimental method can be found in refs. [5, 12], therefore, we only mention here information that is directly relevant to this study.

The samples and monitors used in this study are natural zirconium (99.99%, 100 μm thick) and copper (99.9999%, thickness 55 μm) foils. Zr, Cu, and some other metal foils such as Al (50 μm thick), W (50 μm thick), Pd (100 μm thick) and Y (25 μm thick) used as energy degraders with the same size of 10 mm \times 10 mm were stacked together for simultaneous irradiation. During irradiation, the foil-stack is mounted on a fixed sample holder. The distance between the window of the cyclotron and the foil-stack is 3 cm. A detailed arrangement of the foil-stack for irradiation is shown in Fig. 1.

The irradiation was performed for 1 h with the collimated 45 MeV proton beam with 100 nA and 10 mm beam diameter at the MC-50 cyclotron of the Korea Institute of Radiological and Medical Sciences (KIRAMS) [13]. The average proton energy corresponding to each foil in a

stack was calculated using the SRIM-2013 code [14, 15]. It is known that the SRIM is a software package concerning the stopping and range of ions in matter. It has been continuing upgraded since its introduction in 1985. In calculations, the proton energy loss resulting from passing through the 200 μm aluminum window of the accelerator was also taken into account. It should be noted that the proton energy entering each foil in the stack was calculated in the middle of that foil. For the current arrangement of the foil-stack, the energies of the proton beam in the first and ninth zirconium foils were calculated to be 43.61 MeV and 10.58 MeV, respectively. As the energy spread of the proton beam increases with the thickness of the absorber, the corresponding values of energy spread for the first and ninth zirconium foils also increase from ± 0.37 MeV to ± 1.32 MeV.

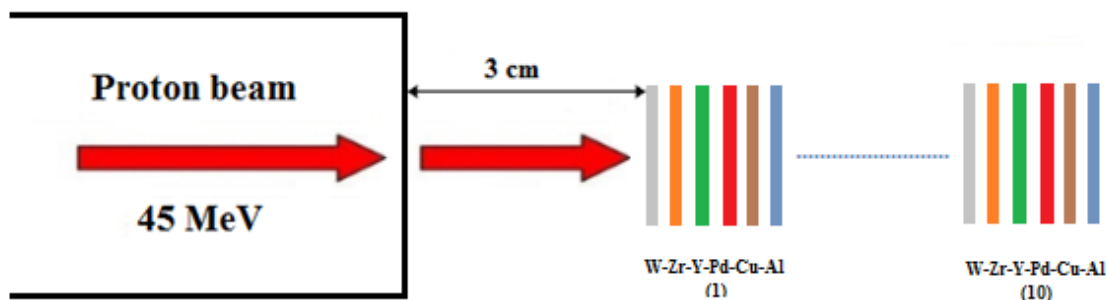


Fig. 1. Layout of the stacked-foil for irradiation on MC-50 cyclotron.

After the irradiation, the activity of residual nuclides produced from both zirconium samples and copper monitors were measured using the same γ -ray spectrometer. It consists of a high-energy resolution γ -ray detector, HPGe (model ORTEC-GEM-20180-p), coupled with a 4096 multi-channel analyzer and associated electronics. The energy resolution of the HPGe detector was 1.8 keV at the 1332.5 keV γ -ray of the ^{60}Co , and the detection efficiency was 20% compared to the 3" \times 3" NaI (TI) detector. The efficiency of the HPGe γ -ray detector was calibrated using standard γ -ray sources of ^{241}Am , ^{137}Cs , ^{60}Co and ^{133}Ba . To support the calibration of activities for residual nuclides measured at different distances between the sample and detector, the efficiency curves at different distances were also determined.

In order to reduce the counting losses due to coincidence summing and pulse pile-up effects, dead time was kept below 5% for all measured γ -ray spectra by choosing appropriate distance between the sample and detector. Depending on the activity and waiting time, irradiated foils should be counted at a distance of 5, 10, or 15 cm from the surface of the HPGe γ -ray detector. Due to the half-lives of residual nuclides of interest are relatively long, activity measurements were performed several times to follow the decay of the radionuclides and to verify the measured results at different waiting times. In this work, some spectra were measured at a waiting time of several tens of hours. The long waiting time not only improves radiation safety but also reduces the Compton background of the γ -ray spectrum. The partial gamma ray spectra of the irradiated zirconium and copper foils are shown in Fig. 2 and Fig. 3, respectively.

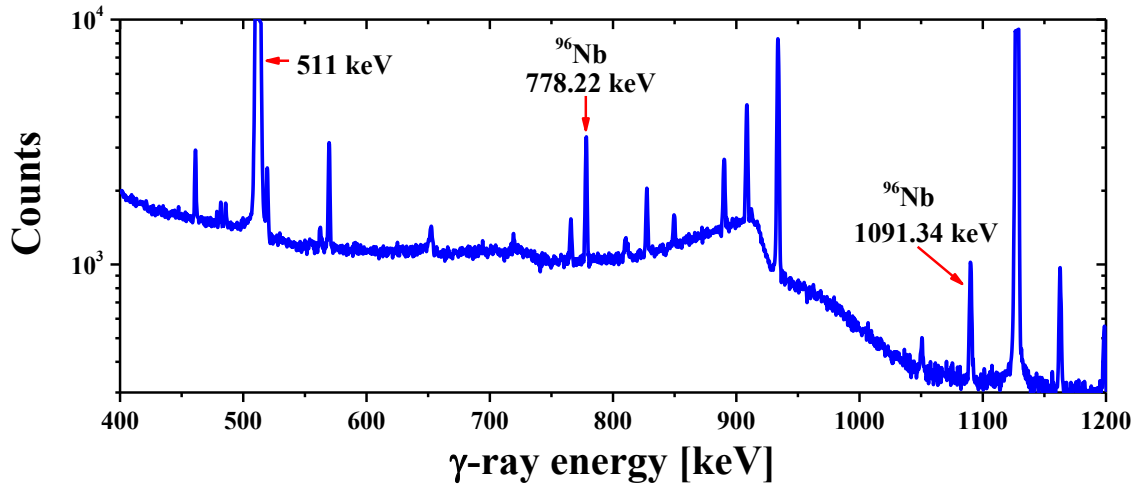


Fig. 2. Partial γ -ray spectrum of natural zirconium foil irradiated by 10.58 MeV proton beam with $t_{ir} = 1$ h, $t_w = 40$ h and $t_m = 20$ min. The γ -peaks of ^{96}Nb used to measure its activity are also displayed.

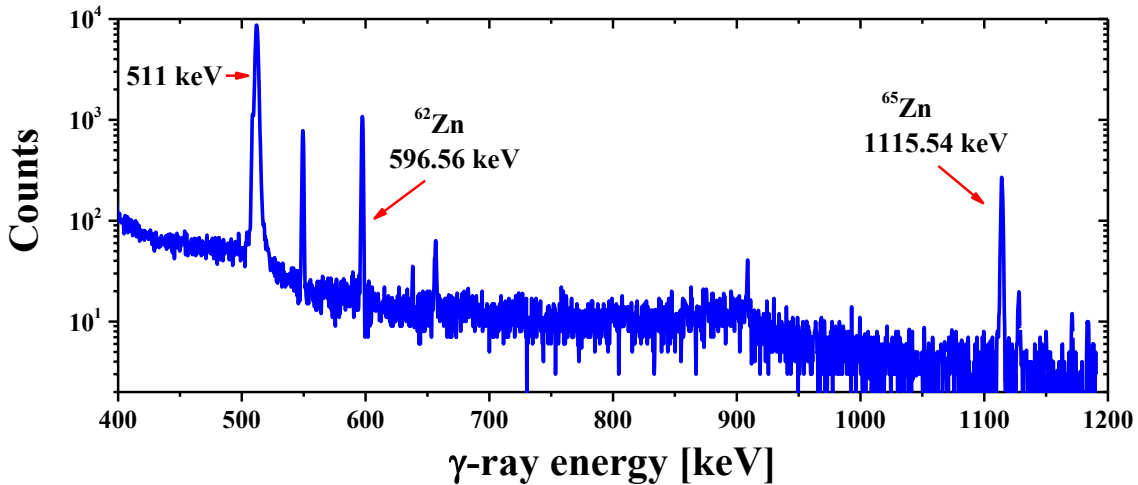


Fig. 3. Partial γ -ray spectrum from natural copper foil irradiated by proton beam with $t_{ir} = 1$ h, $t_w = 20$ h and $t_m = 10$ min. The main γ -peaks of ^{62}Zn and ^{65}Zn formed on $^{\text{nat}}\text{Cu}(p,x)$ reactions are displayed.

All measured γ -ray spectra were analyzed using GammaVision software, version 5.10 (EG&G, ORTEC), which could determine the γ -ray energy and photo-peak area. The appearance of each radionuclide was identified by its characteristic γ -ray energies and half-life. The cross section of the reaction can be deduced from the measured activity of the reaction product after making the necessary corrections. The cross section σ of the $^{\text{nat}}\text{Zr}(p,x)^{96}\text{Nb}$ reaction was

computed based on the activation formula:

$$\sigma = \frac{\lambda S}{N_0 \phi_p \varepsilon_\gamma I_\gamma f_\gamma (1 - e^{-\lambda t_{ir}}) (e^{-\lambda t_w}) (1 - e^{-\lambda t_m})} \quad (1)$$

where λ is the decay constant, S is the photo-peak area of the selected γ -ray, N_0 is the number of target nuclei, ϕ_p is the proton beam flux, ε_γ is the absolute efficiency of the detector at the given γ -ray energy, I_γ is the branching ratio of the measured γ -ray, f_γ denotes the correction factors for counting losses due to γ -ray attenuation and coincidence summing effects [12], and t_{ir} , t_w , and t_m are the irradiation, waiting, and counting times, respectively.

In order to determine the cross section as expressed in Eq. (1) the proton flux was measured using the $^{nat}\text{Cu}(p,x)^{65}\text{Zn}$ and $^{nat}\text{Cu}(p,x)^{62}\text{Zn}$ monitor reactions, where the cross-sections of these two monitor reactions were taken from the reference recommended by the IAEA [16]. The nuclear reactions and the decay data of the product nuclei used in this experiment are presented in Table 1. The decay data are taken from the NuDat database, version 2.8 [17]. Studies show that although natural zirconium consists of five stable isotopes, namely ^{90}Zr (51.45%), ^{91}Zr (11.22%), ^{92}Zr (17.15%), ^{94}Zr (17.38%) and ^{96}Zr (2.80%), but ^{96}Nb can only be produced in the $^{96}\text{Zr}(p,n)^{96}\text{Nb}$ reaction.

Generally, the activity of residual nuclides was measured using the γ -ray(s) of relatively high intensity, interference-free or the interference could be corrected. In the present work, the activity of ^{62}Zn was measured using the γ -ray of 596.56 keV and that of ^{65}Zn was measured using the γ -ray of 1115.54 keV. For the ^{96}Nb residual nuclide, its activity was measured from both 778.22 keV (96.45%) and 1091.34 keV (48.5%) γ -rays.

Table 1. Decay data of the ^{96}Nb , ^{65}Zn and ^{62}Zn radionuclides and their γ -rays were used to calculate the activity [17].

Radio-nuclide	Spin, J_π	Decay mode (%)	Half-live	Main γ -rays, E_γ (keV)	γ -ray intensity, I_γ (%)	Contributing reactions	Thres. energy (MeV)
^{96}Nb	6+	β^- : 100%	23.35 h	778.22 1091.34	96.45 48.5	$^{96}\text{Zr}(p,n)$	0.62
^{65}Zn	5/2-	ε :100%	243.934 d	1115.54	50.4	$^{nat}\text{Cu}(p,x)$	2.17
^{62}Zn	0+	ε :100%	9.193 d	596.56	26.0	$^{nat}\text{Cu}(p,x)$	13.48

It should be noted that, when zirconium targets are bombarded by protons with energies greater than about 20 MeV, the radionuclides ^{96g}Y ($t_{1/2} = 14.74$ h) [17] can be formed through the possible reactions $^{nat}\text{Zr}(p,x)^{86g}\text{Y}$ [10]. The radionuclides ^{86g}Y emit a number of gamma rays, including 777.37 keV (22.4%), which interferes with the 778.22 keV γ -peak of ^{96}Nb . Typical γ -ray spectrum of natural zirconium foil irradiated with 22.47 MeV proton beam can be seen in Fig. 4, in which some γ -peaks of interest such as the 1076.63 keV (82.5%) from ^{86g}Y and the common peak of 777.37-778.22 keV are also displayed. In data analysis, the contribution of the 777.37 keV (22.4%) γ -rays to the common peak of 777.37-778.22 keV can be deduced from the

1076.63 keV (82.5%) γ -peak as follows [5]:

$$S_{777.37\text{keV}} = S_{1076.63\text{keV}} \times \frac{\varepsilon_{777.37\text{keV}} \times I_{777.37\text{keV}}}{\varepsilon_{1076.63\text{keV}} \times I_{1076.63\text{keV}}} \quad (2)$$

where S , ε and I represent the photo-peak area, detector efficiency and γ -ray intensity with energies of 777.37 keV and 1076.63 keV, respectively.

Further corrections to be considered are γ -ray attenuation and true coincidence summing effects. The attenuation factors of the γ -rays used, namely 596.56 keV and 1115.54 keV in copper foil and 778.22 keV and 1091.34 keV in zirconium foil were calculated to be around units. In addition, for a given measurement arrangement, namely 10 cm between the sample and the detector, the true coincidence summing effect for both 778.22 keV and 1091, 34 keV γ -rays is negligible small. So, in practice, no correction is necessary for both effects.

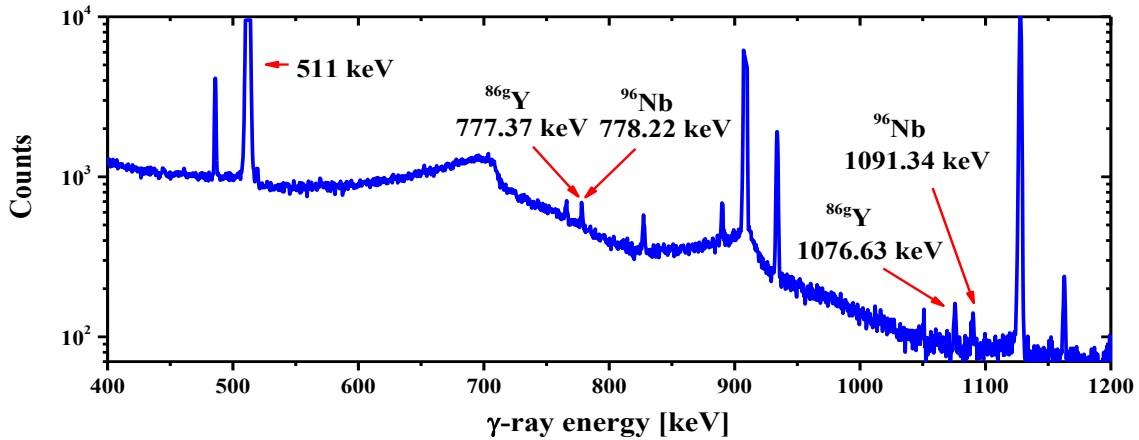


Fig. 4. Partial γ -ray spectrum of natural zirconium foil irradiated by 22.47 MeV proton beam with $t_{ir} = 1$ h, $t_w = 40.5$ h and $t_m = 20$ min. The γ -rays of interest emitted from ^{96}Nb and ^{86g}Y are also displayed.

III. MODEL CALCULATIONS

The excitation function of the $^{\text{nat}}\text{Zr}(p,x)^{96}\text{Nb}$ reaction was calculated using the latest TALYS-1.95 code [18]. The TALYS code is a comprehensive computer code that can be used to analyze and predict nuclear reactions involving light ions, including protons in the energy range 0.001 to 200 MeV and on target nuclei with mass number in the range from 24 to 250. This code allows calculations of the cross section in this energy range based on theoretical models for compound, direct and pre-equilibrium reactions. TALYS-1.95 [18] updates latest versions of almost theoretical models (for nuclear structure and nuclear reaction) and have been verified with current experimental nuclear data library. TALYS code allows the user choices among different available models for specific task and many options for each model. Therefore, the TALYS code is a good tool for studying theoretical nuclear reactions. However, in order to improve the computer code, experimental cross-section data are essentially important.

In this work, TALYS code was run with all stable isotopes of Zr element but there has only reaction channel of ^{96}Zr isotope formed ^{96}Nb . The total cross section of the $^{96}\text{Zr}(p,n)^{96}\text{Nb}$ reaction was calculated based on the contributions of the compound, direct and equilibrium reaction processes. For further study, the calculations were tested with six different level density options, namely the constant temperature Fermi gas model (CTFGM), back-shifted Fermi gas model (BSFGM), generalized superfluid model (GSFM), microscopic nuclear level density (Skyrme force) from Goriely's table (SFGM), microscopic nuclear level density (Skyrme force) from Hilaire's combinatorial tables (SFHM), and microscopic nuclear level density (temperature dependent HFB, Gogny force) from Hilaire's combinatorial tables (GFHM). Details of the calculations were described elsewhere [5, 19]. The calculated results in the energy range up to 60 MeV with six level density options are shown in Fig. 5.

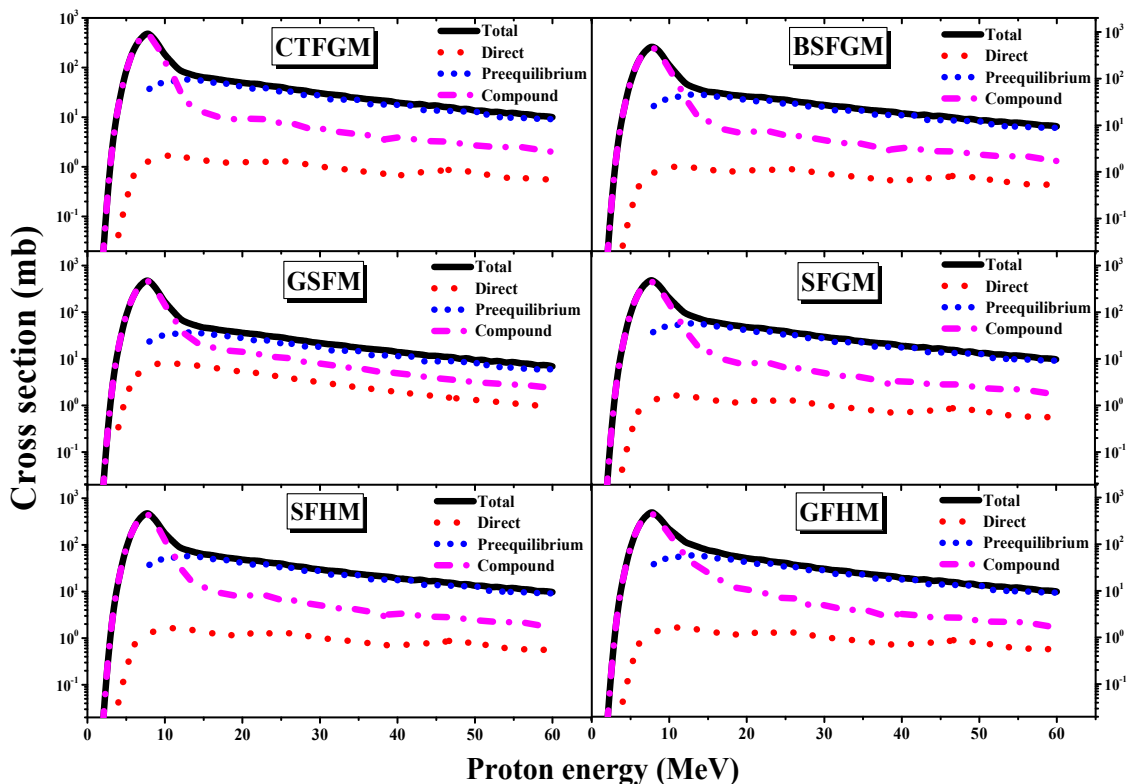


Fig. 5. The contribution of compound, direct and pre-equilibrium components to the excitation function of $^{96}\text{Zr}(p,n)^{96}\text{Nb}$ reaction with 6 models of nuclear level density.

As can be seen in Fig. 5, the compound mechanism contributes greatly to the formation of the $^{96}\text{Zr}(p,n)^{96}\text{Nb}$ reaction, while the pre-equilibrium and the direct mechanism contribute smaller fractions, starting from energies of about 4 and 7 MeV, respectively. Based on this calculation and the abundance of natural zirconium isotopes, the cross section of the $^{\text{nat}}\text{Zr}(p,x)^{96}\text{Nb}$ reaction was derived and compared with the experimental results.

IV. RESULTS AND DISCUSSIONS

The measured cross sections of the $^{\text{nat}}\text{Zr}(p,x)^{96}\text{Nb}$ reaction as a function of proton energy are given in Table 2. Each cross section value is averaged over several measured results. As presented in our recent publication [5] the uncertainties of the experimental cross sections were determined from the square root of the sum in quadrature of the main source uncertainties such as the counting statistics (3–5%), the nuclear data used (2–4%), the detector efficiency calibration (3–5%), the fitting of photo-peak area (3–4%), the variation of proton beam (5–8%), the cross section extracted from the standard reactions (4–5%) and the possible other error sources could not be identified (4–6%). Thus, the total uncertainties of the measured cross-sections are expected in the range of 9–15%.

Table 2. Experimental cross sections as a function of proton energy for the $^{\text{nat}}\text{Zr}(p,x)^{96}\text{Nb}$ reaction.

Proton energy (MeV)	Cross section (mb)
43.61 ± 0.37	0.25 ± 0.03
40.70 ± 0.41	0.42 ± 0.06
37.60 ± 0.44	0.41 ± 0.06
34.33 ± 0.50	0.58 ± 0.08
30.76 ± 0.54	0.59 ± 0.08
26.87 ± 0.63	0.63 ± 0.08
22.47 ± 0.72	1.33 ± 0.16
17.30 ± 0.88	1.26 ± 0.15
10.58 ± 1.32	6.21 ± 0.90

For comparison, the current measured cross-sections are plotted in Fig. 6 together with previously measured data [6–11], six excitation functions predicted by TALYS-1.95 [18] code using six different level density models and the theoretical data taken from the TENDL-2019 library [20]. As can be seen, all the excitation functions predicted in theory calculations are in fairly good agreement with each other. In general, the reported cross-sectional data reproduce the shape of the theoretical prediction excitation functions, and most of the measured data agree with the magnitude of the theoretical predictions, except for the values reported by Tarkanyi *et al.* [7] and Uddin *et al.* [10] overestimated above 20 MeV. From Fig. 6 we can also see that, the currently measured cross sections are lower than those of Tarkanyi *et al.* [7] in the energy range above 20 MeV and Uddin *et al.* [10] in the energy range of 30 - 40 MeV, but are in good agreement with the data measured by Al-Abyad *et al.* [9] in the energy range of 10 - 15 MeV, Szelecsenyi *et al.* [6] and Michel *et al.* [11] in the energy range of 10 – 45 MeV. In addition, the present results are consistent with the theoretical predictions using the TALYS-1.95 [18] code calculated for all six level density models and with the data from TENDL-2019 library [20] over the entire energy range studied.

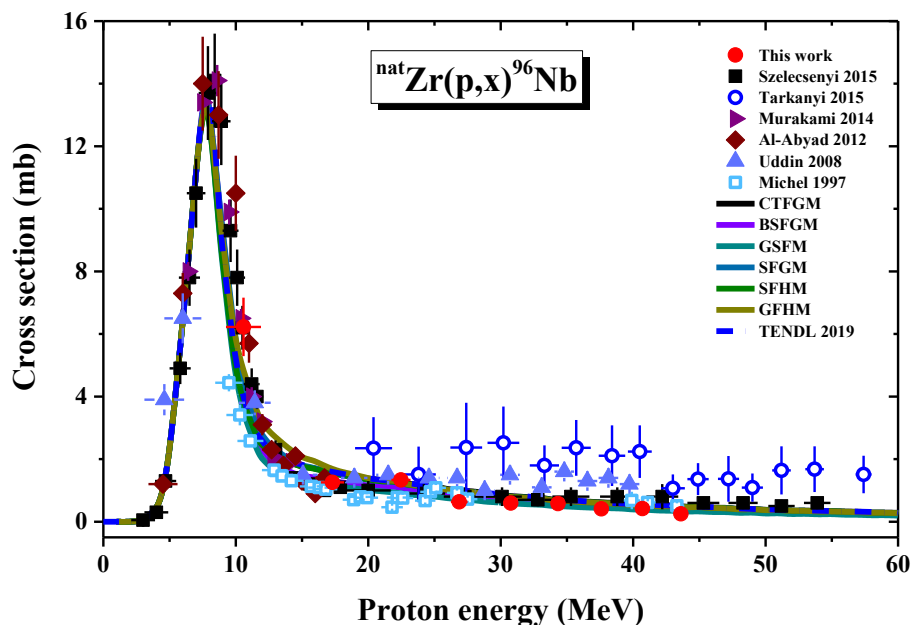


Fig. 6. Measured and calculated cross sections as a function of proton energy for the ${}^{\text{nat}}\text{Zr}(p,x){}^{96}\text{Nb}$ reaction.

V. CONCLUSIONS

The excitation function of the ${}^{\text{nat}}\text{Zr}(p,x){}^{96}\text{Nb}$ reaction was measured in the proton energy range from 10.58 to 43.61 MeV by a stacked-foil activation technique combined with off-line γ -ray spectroscopy. In this experiment, appropriate γ -ray spectrum measurements and data processing procedures were made to accurately determine the activities of residual nuclei. The excitation function for the ${}^{\text{nat}}\text{Zr}(p,x){}^{96}\text{Nb}$ reaction was also calculated using the TALYS-1.95 code [18]. For the calculation, all three reaction processes including compound, direct and pre-equilibrium were taken into account. The present results are in good agreement with most of the recent measured data [6, 9, 11] and the theoretical predictions using the code TALYS-1.95 [18] and TENDL-2019 [20] data library in whole studied energy range.

ACKNOWLEDGEMENTS

The authors express their sincere thanks to the Korea Institute of Radiological and Medical Sciences (KIRAMS), Korea and staff of the MC-50 Cyclotron Laboratory for the valuable support to carry out this experiment. This research work is supported in part by the Vietnam National Foundation for Science and Technology Development (NAFOSTED) under Grant No. 103.04-2018.314.

REFERENCES

- [1] I. Dillmann, L. Coquard, C. Domingo-Pardo, F. Kappeler, J. Marganiec, E. Uberseder, U. Giesen, A. Heiske, G. Feinberg, D. Hentschel, S. Hilpp, H. Leiste, T. Rauscher, F.-K. Thielemann, *Phys. Rev. C* **84** (2011) 015802.

- [2] H. Zaneb, M. Hussain, N. Amjed, S.M. Qaim, *Appl. Radiat. Isot.* **104** (2015) 232.
- [3] Syed M. Qaim, Ingo Spahn, Bernhard Scholten, and Bernd Neumaier, *Radiochim. Acta* **104** (2016) 601.
- [4] B.M. Ali, M. Al-Abyad, S. Kandil, A.H.M. Solieman, and F. Ditroi, *Eur. Phys. J. Plus* **133** (2018) 9.
- [5] N. V. Do, N. T. Luan, N. T. Hien, G. N. Kim, N. T. Xuan, K. T. Thanh, *Eur. Phys. J. A* **56** (2020) 194.
- [6] F. Szelecsenyi, G.F. Steyn, Z. Kovacs, C. Vermeulen, K. Nagatsu, M.-R. Zhang and K. Suzuki, *Nucl. Instr. Meth. B* **343** (2015) 173.
- [7] F. Tarkanyi, F. Ditroi, S. Takacs, A. Hermanne, M. Al-Abyad, H. Yamazaki, M. Bada and M.A. Mohammadi, *Appl. Radiat. Isot.* **97** (2015) 149.
- [8] M. Murakami, H. Haba, S. Goto, J. Kanaya and H. Kudo, *Appl. Radiat. Isot.* **90** (2014) 149.
- [9] M. Al-Abyad, A.S. Abdel-Hamid, F. Tarkanyi, F. Ditroi, S. Takacs, U. Seddik and I. I. Bashter, *Appl. Radiat. Isot.* **70** (2012) 257.
- [10] M.S. Uddin, M.U. Khandaker, K.S. Kim, Y.S. Lee, M.W. Lee and G.N. Kim, *Nucl. Instr. Meth. B* **266** (2008) 13.
- [11] R. Michel, R. Bodemann, H. Busemann, R. Daunke, M. Gloris, H.-J. Lange, B. Klug, A. Krins, I. Leya, M. Luepke, S. Neumann, H. Reinhardt, M. Schnatz-Buettgen, U. Herpers, Th. Schiekkel, F. Sudbrock, B. Holmqvist, H. Conde, P. Malmberg, M. Suter, B. Dittrich-Hannen, P.-W. Kubik, H.-A. Sinal and D. Filges, *Nucl. Instr. Meth. B* **129** (1997) 153.
- [12] N. V. Do, N. T. Luan, N. T. Xuan, N. T. Hien, G. N. Kim, K. S. Kim, *J. Radioanal. Nucl. Chem.* **321** (2019) 117.
- [13] M. U. Khandaker, A. K. M. M. H. Meaze, K. S. Kim, D. C. Son, G. N. Kim, *J. Korean. Phys. Soc.* **48** (2006) 821.
- [14] J. F. Ziegler, SRIM-2003. *Nucl. Instr. Meth. B* **219–220** (2004) 1027.
- [15] J. F. Ziegler, J. P. Biersack, U. Littmark (2003) SRIM 2003 code, Version 96.xx. The Stopping and Range of Ions in Solids. Pergamon, New York, available from <http://www.srim.org/>.
- [16] S.M. Qaim, F. Tárkányi, P. Obložinský, K. Gul, A. Hermanne, M.G. Mustafa, F.M. Nortier, B. Scholten, Y. Shubin, S. Takács, Y. Zhuang, IAEA-TECDOC-1211, Vienna (2001). Available from <http://www.nds.iaea.org/medical/>.
- [17] Nudat 2.8, National Nuclear Data Center, Brookhaven National Laboratory, available from <http://www.nndc.bnl.gov/nudat2/>.
- [18] A. Koning, S. Hilaire and S. Goriely, TALYS-1.95, a nuclear reaction program, NL-1755 ZG Petten the Netherlands (2019). Available from https://tendl.web.psi.ch/tendl_2019/talys.html.
- [19] Ozan Artun, *Appl. Radiat. Isot.* **144** (2019) 64.
- [20] TENDL-2019: TALYS-based evaluated nuclear data library (2019). Available from https://tendl.web.psi.ch/tendl_2019/tendl2019.html.